Ion Implantation

Instructor: Dr. M. Razaghi

Comparison of (a) diffusion and (b) ion-implantation techniques for the selective introduction of dopants into the semiconductor substrate.

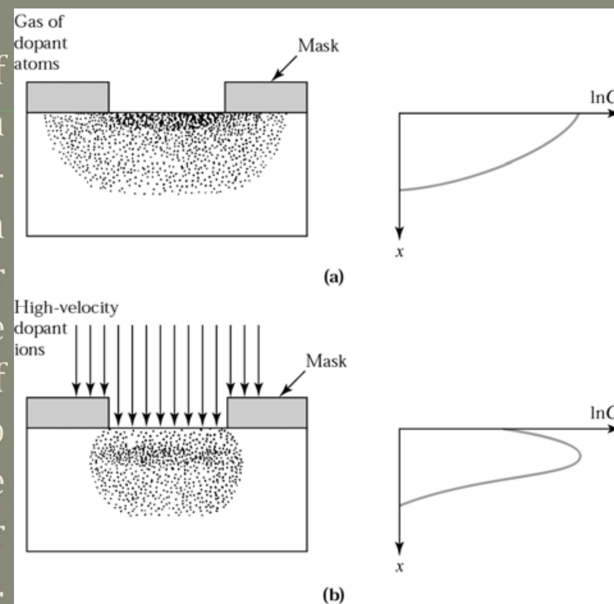

Instructor: Dr. M. Razaghi

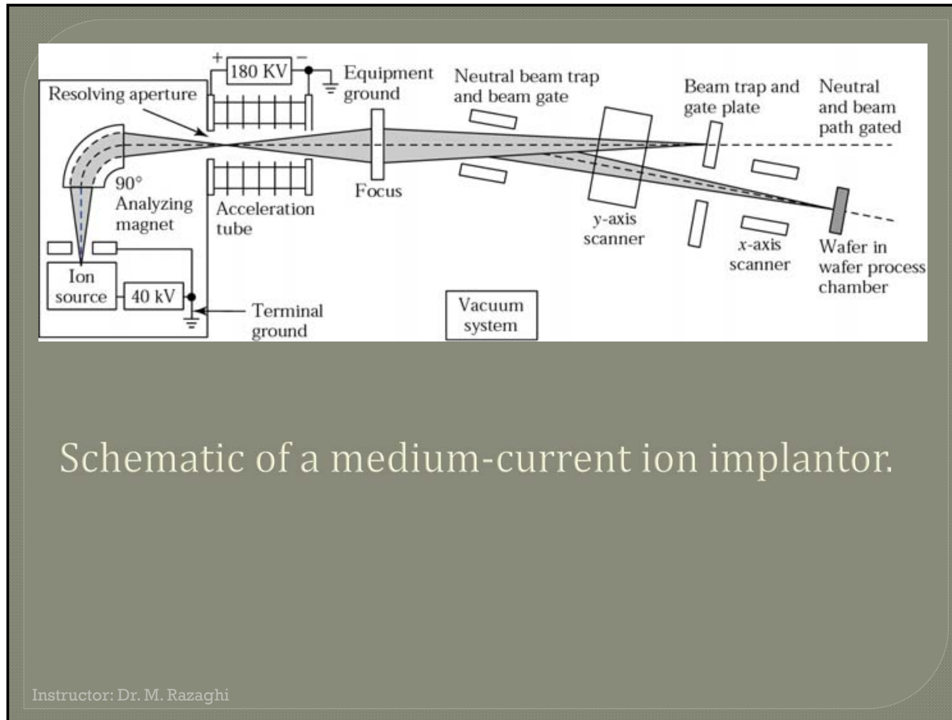
180 KV
Equipment ground
Neutral beam trap and beam gate
Beam trap and gate plate
Neutral and beam path gated
Resolving aperture
90° Analyzing magnet
Acceleration tube
Focus
y-axis scanner
x-axis scanner
Wafer in wafer process chamber
Ion source
40 kV
Terminal ground
Vacuum system
Schematic of a medium-current ion implantor.
Instructor: Dr. M. Razaghi

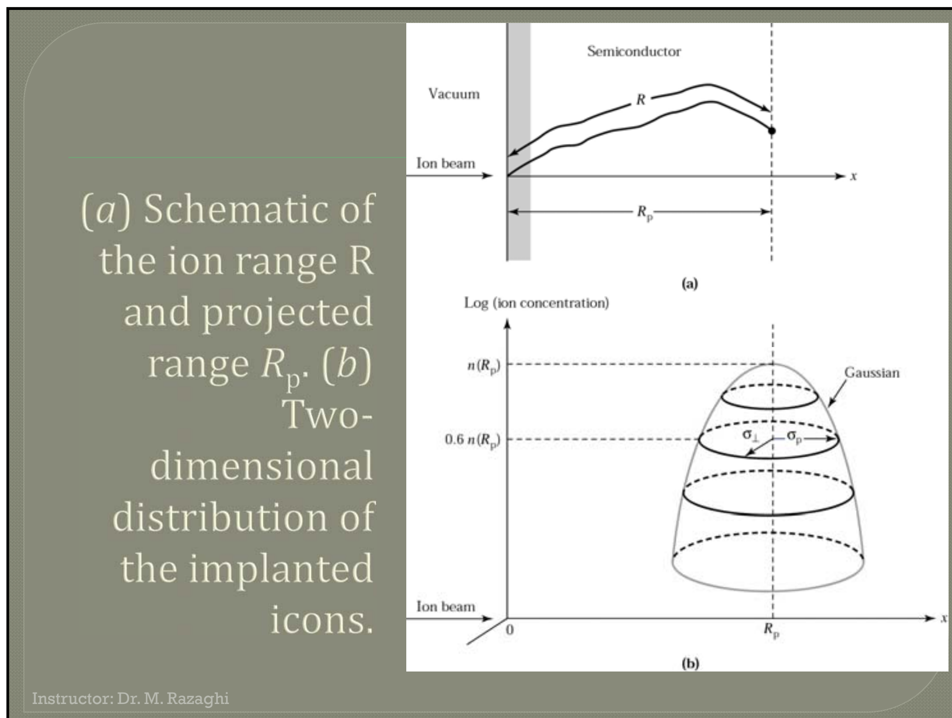
Semiconductor
Vacuum
R
Ion beam
x
R_p
(a)
Log (ion concentration)
$n(R_p)$
Gaussian
$0.6\ n(R_p)$
$\sigma_\perp$
σ_p
Ion beam
0
R_p
x
(b)
(a) Schematic of the ion range R and projected range R_p. (b) Two-dimensional distribution of the implanted icons.
Instructor: Dr. M. Razaghi

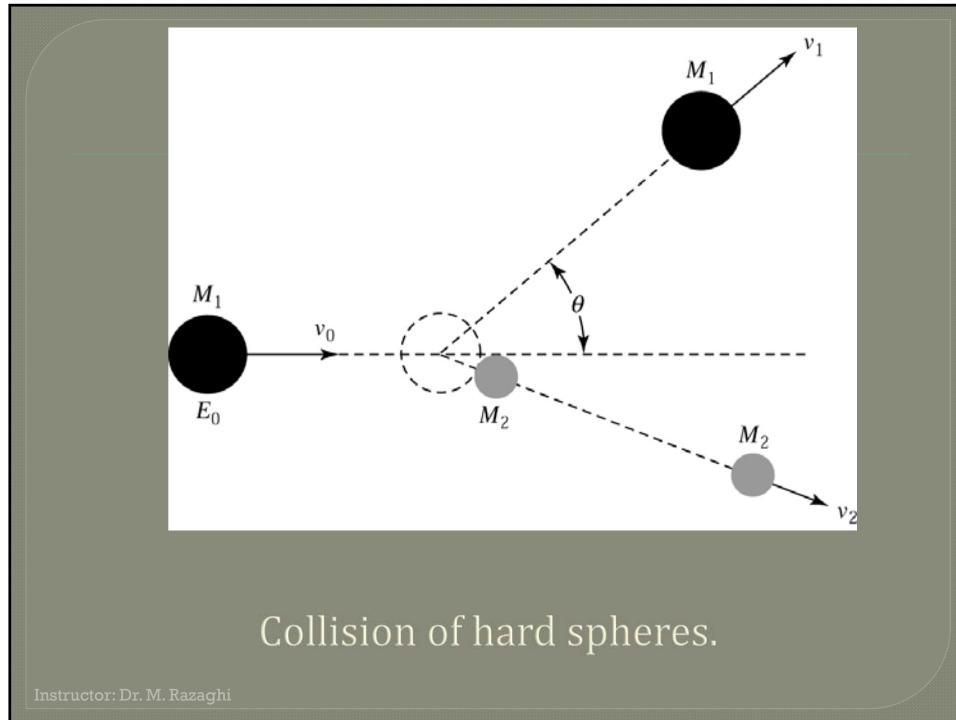

Collision of hard spheres.

Instructor: Dr. M. Razaghi

Nuclear stopping power, Sn(E) and electronic stopping power, $S_e(E)$ for As, P, and B in Si. The points of intersection of the curves correspond to the energy at which nuclear and electronic stopping are equal.

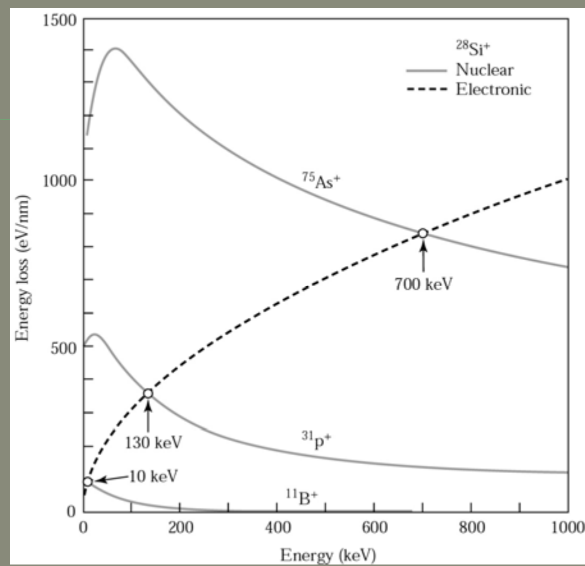

Instructor: Dr. M. Razaghi

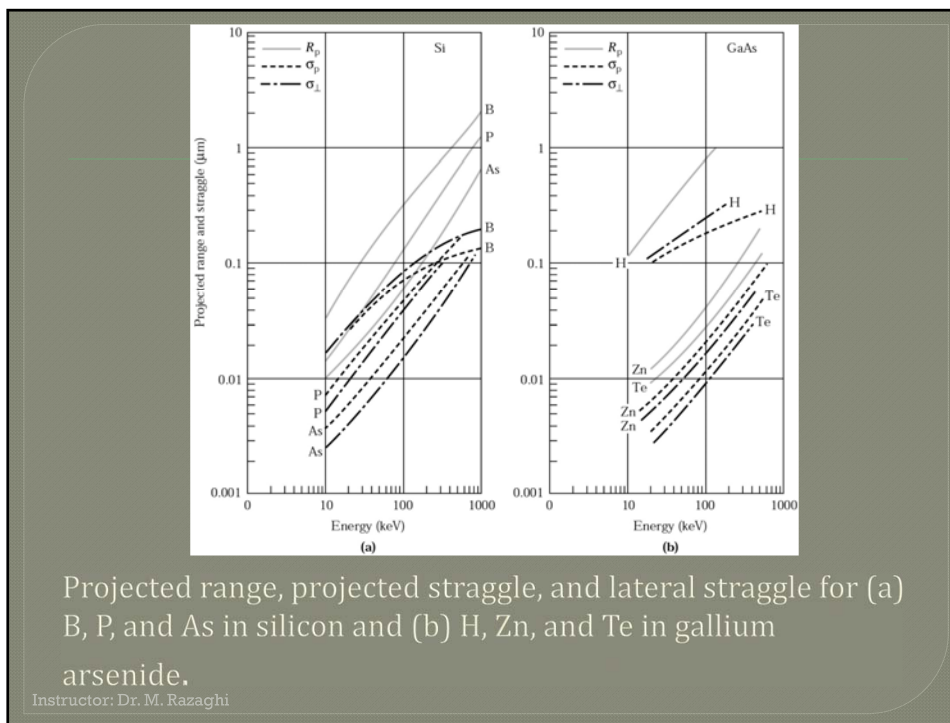

Projected range, projected straggle, and lateral straggle for (a) B, P, and As in silicon and (b) H, Zn, and Te in gallium arsenide.

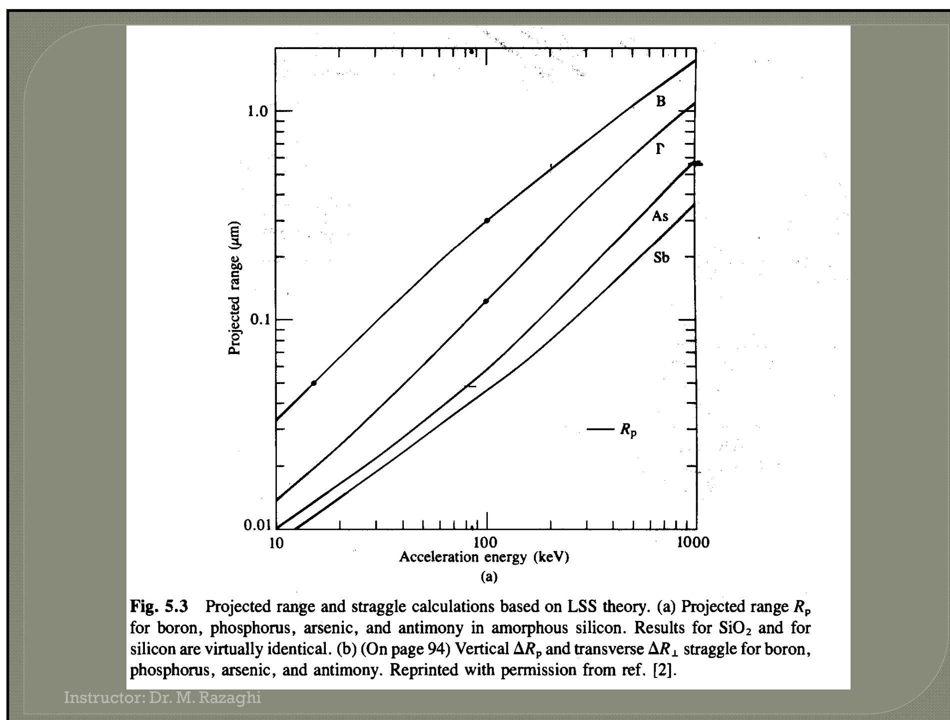

Fig. 5.3 Projected range and straggle calculations based on LSS theory. (a) Projected range R_p for boron, phosphorus, arsenic, and antimony in amorphous silicon. Results for SiO_2 and for silicon are virtually identical. (b) (On page 94) Vertical ΔR_p and transverse $\Delta R_\perp$ straggle for boron, phosphorus, arsenic, and antimony. Reprinted with permission from ref. [2].

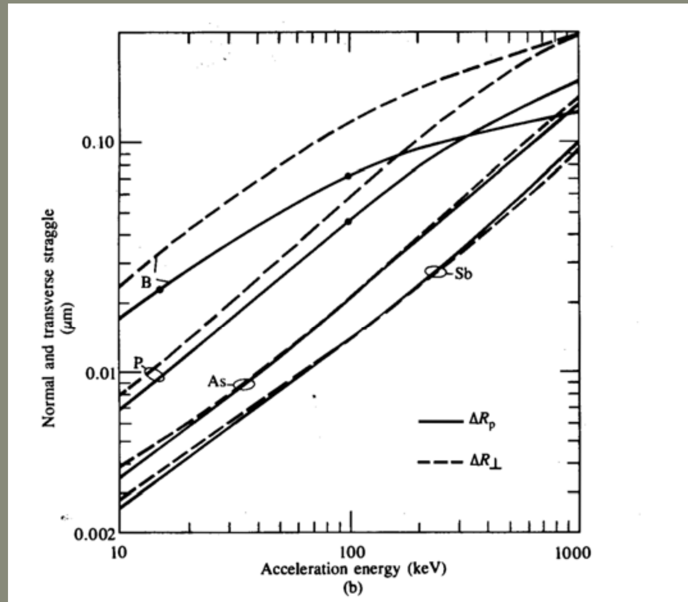

Fig. 5.3 (continued)

Instructor: Dr. M. Razaghi

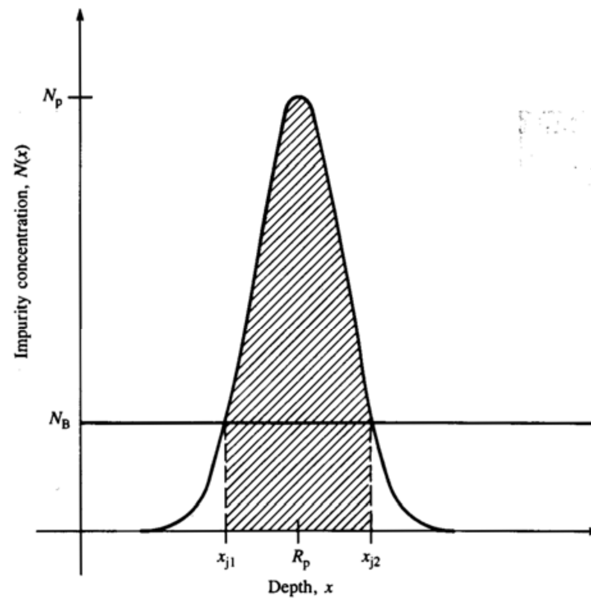

. 5.6 Junction formation by impurity implantation in silicon. Two *pn* junctions are formed x_{j1} and x_{j2}.

Instructor: Dr. M. Razaghi